

# Multiphoton Laser Scanning Microscopy

## Using the Zeiss LSM 510 NLO



*Urechis caupo*  
Serotonin positive nerve cells

Written by Mary Dickinson, PhD  
Biological Imaging Center  
California Institute of Technology  
February 2002





---

## CONTENTS

	Page
<b>8 MULTIPHOTON LASER SCANNING MICROSCOPY .....</b>	<b>8-5</b>
8.1 Preface .....	8-5
8.2 Introduction to Multiphoton Laser Scanning Microscopy .....	8-6
8.2.1 Multiphoton excitation – How does it work? .....	8-6
8.2.2 Increased signal-to-noise, enhanced vitality, and deep optical sectioning in MPLSM .....	8-8
8.2.3 Drawbacks of using NIR light for microscopy .....	8-9
8.2.4 Achieving Efficient Multiphoton Excitation using Ultrafast lasers .....	8-10
8.2.5 Optimizing the Peak Intensity without Frying the Samples .....	8-11
8.3 Using the LSM 510 NLO direct coupled system: Practical considerations for optimal imaging .....	8-13
8.3.1 Coupling the Coherent Mira 900F to the LSM 510 NLO .....	8-13
8.3.2 Using and tuning the Coherent Mira 900F – A simplified protocol for direct-coupled LSM 510 NLO systems .....	8-13
8.3.2.1 Turn on procedure .....	8-14
8.3.2.2 Achieving stable mode-lock .....	8-16
8.3.2.3 Tuning the MIRA 900F to a new wavelength .....	8-17
8.3.2.4 Adjusting the bandwidth of the pulse .....	8-18
8.3.3 Alignment of the Coherent MIRA 900F into the LSM 510 NLO scan head .....	8-19
8.3.3.1 Quick alignment protocol .....	8-19
8.3.3.2 Advanced alignment protocol .....	8-21
8.3.3.3 Tips on maintaining alignment with the scan head .....	8-23
8.3.4 Objectives recommended for Multiphoton Excitation .....	8-23
8.3.5 Choosing Fluorescent Probes for MPLSM .....	8-25
8.3.6 Samples your mother should have warned you about .....	8-27
8.4 Troubleshooting Checklist .....	8-30
8.4.1 No image being produced .....	8-30
8.4.2 Poor image quality .....	8-31
8.5 References .....	8-33

MULTIPHOTON LASER SCANNING MICROSCOPY  
Contents

Carl Zeiss

LSM 510 NLO

---

## **8 MULTIPHOTON LASER SCANNING MICROSCOPY**

### **8.1 Preface**

Safety Considerations when using ultrafast lasers coupled to a microscope.



Users operating ultrafast lasers have to observe all of the precautions specified in the Operating Manual for the laser and caution should be exercised when using the laser.



All users should be familiar with risks and good safety practices before access to the laser is granted.



Users must not look directly into the laser beam. Direct eye contact with the output beam from the laser will cause serious damage and possible blindness.



Every precaution should be taken to avoid exposing skin, hair or clothing to the laser, as this may cause burns.



Beware of reflected laser light and remove jewelry before working with the laser.



Avoid using organic solvents near the laser.



Protective housings should remain in place, when the laser is in use.



Safety signs have to be posted to inform people that lasers may be in use.

## 8.2 Introduction to Multiphoton Laser Scanning Microscopy

Multiphoton laser scanning microscopy (MPLSM) has become an important technique in vital and deep tissue fluorescence imaging. In MPLSM, fluorescent molecules are excited by the simultaneous absorption of two or more near infrared (NIR) photons. Multiphoton excitation has a quadratic dependence, producing excitation only at the focal plane; thus, out-of-focus fluorescence does not contribute to image background, and photodamage outside the plane of focus is greatly reduced. In practical terms, MPLSM makes it possible to acquire images with a high signal-to-noise ratio by using a wavelength that is less harmful to live cells. The use of NIR light makes it possible to image deeper in the specimen, due to less scatter and absorption of the incident light. However, multiphoton excitation depends on some special criteria that differ from those needed for single photon excitation events. Here we will provide a simplified explanation of the physics of multiphoton excitation.

### 8.2.1 Multiphoton excitation – How does it work?

In single photon excitation, a fluorescent molecule or fluorochrome (also called a chromophore) absorbs a high energy photon of light within a certain wavelength range and then, within nanoseconds, releases a photon of longer wavelength (lower energy). The absorption of a photon results in the excitation of the molecule, by displacing an electron within the molecule from the ground state to an excited state. Thus, for a single photon excitation event, excitation is directly proportional to the incident photon flux of the source, since each photon has an equal probability of exciting a molecule in the ground state. As the molecule relaxes back to the ground state, some energy is lost through non-radiative exchange (heat or vibration within the molecule), but the rest is shed as a photon of light.

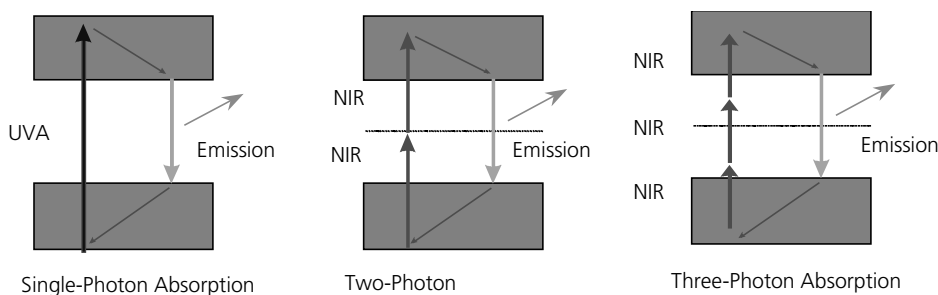


**Fig. 8-1 The principle of multiphoton excitation**

The energy loss accounts for the Stokes shift seen between the excitation and the emission wavelength and explains why the emission maxima is always of a lower energy, more red-shifted, from the excitation maxima. Multiphoton excitation of the fluorochrome is induced by the combined effect of two or more, lower energy, NIR photons. As a rule of thumb the energy of the two photons is roughly half the energy of the photons needed for single photon absorption, although there are clear exceptions to this rule. Multiphoton excitation can be achieved by two photons of the same or different wavelengths, but with a single laser source, two photons of the same wavelength are used.

The probability of multi-photon excitation is proportional to the incident photon flux density which is the intensity squared ( $I^2$ ), because a quasi-simultaneous absorption of two photons is necessary. It follows, that for three-photon excitation, the probability of three-photon absorption is the intensity cubed ( $I^3$ ). The emission characteristics of the excited fluorochrome is unaffected by the different absorption processes (Fig. 8-1).

While this appears conceptually simple, two difficulties, at the level of the fluorochrome, confound our understanding of this process. First, it is difficult to predict whether a molecule will efficiently absorb the two lower energy photons simultaneously. Drastic differences in multiphoton absorption between different molecules have been identified and it is difficult to predict by the structure of a molecule how well it will efficiently absorb simultaneous low energy photons, although some theories are emerging (see Albota et al., 1998; Rumi et al., 2000 for review). Second, the wavelengths for maximum multiphoton excitation are very difficult to predict. Deriving the multiphoton excitation wavelength maximum is clearly not as simple as doubling the single photon excitation wavelength maximum. Both of these criteria must be measured and are reflected in the multiphoton cross-section (usually referred to as  $\delta$ ) for a given fluorochrome (see Xu, 2000 for review).

The cross-section data indicate how well the molecule absorbs multiphoton energy at different wavelengths of NIR light. What is both interesting and perplexing about this data is that several molecules that all emit green light, i.e. excited at roughly the same wavelength via single photon absorption, can have multiphoton excitation maxima that are very different. For instance, although Fluorescein and GFP both emit green light, the multiphoton cross-section peak for Fluorescein is 770-790 nm, but is centered around 900 nm for GFP (S65T) (Xu, 2000) whereas, the single photon excitation maxima for these two molecules are both around 470-490 nm. These questions represent an intense area of investigation for physicists and chemists who specialize in multiphoton absorption (see Section 8.3.5 Choosing fluorescent probes for MPLSM).

### 8.2.2 Increased signal-to-noise, enhanced vitality, and deep optical sectioning in MPLSM

One of the greatest benefits of multiphoton excitation is that excitation is practically limited to the focal plane. This effect increases signal-to-noise and decreases phototoxicity. In single photon excitation, the excitation of a dye is directly proportional to the average power ( $Ex \sim P_{avg}$ ). Thus, excitation takes place in the whole cone of focus and optical resolution is accomplished by using a confocal aperture. For multiphoton excitation, however, excitation of the dye is proportional to the squared intensity ( $Ex \sim I^2$ ), as mentioned above. For a focused beam, intensity ( $I$ ) can be described as average power ( $P_{avg}$ ) divided by the cross-sectional area of the beam ( $A$ ), so for multiphoton excitation, the excitation is proportional to the average power divided by the area of the beam, squared ( $Ex \sim [P_{avg}/A]^2$ ). Thus, as the beam diameter becomes smaller (such as at the focal plane) excitation is increased and excitation out of the plane of focus becomes highly improbable and falls off with the axial distance from the focal plane with the power of 4. This explains why multiphoton excitation is mainly limited to the focal plane (Fig. 8-2). Moreover, the cross-sectional area of the beam is dependent on the NA of the objective. Objectives with a larger NA can focus light to a smaller beam waist, which is why high NA objectives are preferred for multiphoton excitation microscopy.

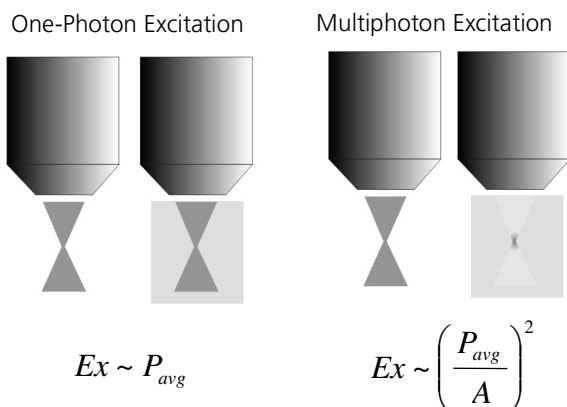


**Fig. 8-2** One-photon vs. Multiphoton excitation. Two images of an objective are shown for each example. In each case, the first indicates the shape of the focused beam after passing through the objective. The second indicates the fluorescence that would be observed if the beam was focused through a cuvette containing a homogeneous solution of fluorescent dye.

Since out-of-focus fluorescence, which usually contributes to background noise in the image, is created inefficiently, MPLSM can be a better technique for imaging fine structures masked by background noise. Optical sectioning can be performed without the use of the pinhole to eliminate out-of-focus fluorescence and nearly all of the fluorescence produced at the plane of focus can be used to make the image. Although a pinhole is not normally needed using MPLSM, it is possible to use the confocal pinhole together with multiphoton excitation to prevent highly scattered photons from reaching the detector and to improve optical sectioning. This can be done on an LSM 510 NLO by carefully adjusting the collimation lens and the z-position of pinhole 1 (Refer to the alignment protocol in subsequent sections).

It is tempting to think of the decrease in background signal as an increase in resolution. This is a common misconception. In fact, due to the longer excitation wavelength the optical resolution along the optical axis is worse in comparison to the resolution in a classical confocal LSM. Objects obscured by background fluorescence, may appear brighter or more defined using MPLSM, but this is not due to an increase in resolution, but rather a reduction in background noise, resulting in better contrast.

The lack of out-of-focus excitation greatly reduces bleaching, and therefore, photodamage, throughout the sample. This reduces damage caused by repeated or slow scans; however, photobleaching at the focal plane is still present. In fact, some reports indicate that bleaching may be accelerated at the plane of focus using multiphoton excitation (Patterson and Piston, 2000). Some essential, endogenous molecules within the cell can absorb UV or visible range photons (such as NAD, FADH etc.), which can destroy and deplete these molecules. Thus, it can be safer for vital imaging to use an excitation source outside of the visible range like a NIR laser. A profound example of this effect is seen in a comparative study performed by Squirrell and colleagues (Squirrell et al. 1999), where the vitality of cleavage stage hamster embryos was assessed after repeated exposure to visible range laser light and pulsed 1047 nm laser light. In these experiments, confocal imaging resulted in arrested cellular division and embryo lethality, whereas imaging using multiphoton microscopy resulted in much less embryo lethality and better data collection. In fact, at least one embryo imaged in this way was able to develop into a completely normal adult hamster named laser, illustrating the strength of this technique.

The use of NIR light has the additional benefit of being able to penetrate deeper into tissue than visible wavelength light. Compared to confocal microscopy, excitation can be achieved in deeper positions of the specimen and more data along the z-axis can be obtained. However, particularly in deep tissue imaging, care must be taken to recover as many emission photons as possible. While the incident NIR light has an advantage over visible range excitation sources, the photons that are emitted are at visible wavelengths and have the potential to be scattered or absorbed by the tissue. To improve the efficiency of collection, high numerical aperture (NA) objectives should be used, although it is often difficult to obtain lenses that have NAs above 1 with a working distance longer than 250  $\mu\text{m}$ . In addition, non-descanned detectors (NDDs), which collect photons at a point closer to the specimen and do not require the emission to be focused back through the scan mechanism, can be used to improve deep tissue imaging by improving the collection efficiency of scattered photons

### **8.2.3 Drawbacks of using NIR light for microscopy**

Although the use of NIR photons has many advantages, there is a distinct disadvantage to this mode of excitation.

Absorption of NIR light by water and some other particular molecules (such as melanocytes or condensed particles such as calcium carbonate crystals) can create dramatic local heating effects within the sample. This effect increases as the overall power from the laser is increased at the sample. It is very important to use minimized power levels to reduce the effects of local heating. For live samples, power levels above 6 mW may disturb cell replication (König et al. 1996) or even cause cells to explode, as in the case of melanocytes in zebrafish embryos. Effects of local heating can not only damage cells, but can also contribute to image artifacts (see Section 8.3.6. Samples your mother should have warned you about). As you will see in the next section, optimizing the pulse length at the specimen can improve multiphoton excitation without raising the average power.

#### 8.2.4 Achieving Efficient Multiphoton Excitation using Ultrafast lasers

In order to achieve efficient two- or three-photon excitation, the photons must collide with the molecule simultaneously. For single-photon excitation, a continuous wave laser with a continuous photon flux can be used because the probability of excitation is directly proportional to the photon flux or average power of the source. Increasing the laser intensity (turning up the power) increases the photons delivered to the sample, increasing excitation until all of the molecules are saturated. To deliver enough photons to achieve simultaneous absorption of two NIR photons using a continuous wave laser would require enormous power. Ultrafast lasers improve the efficiency of multiphoton excitation by delivering photons in pulsed "wave packets". The high peak intensity needed for multiphoton excitation is created by concentrating photons into very brief pulses which are delivered to the sample over and over again at a rapid rate, about every 13 ns, to ensure efficient dye excitation. Instead of a steady flux of photons bombarding the fluorochrome one after another, multiple photons collide with the molecule simultaneously. This process has the advantage of delivering a high peak intensity, to satisfy the  $I^2$  or  $I^3$  requirement for two- or three-photon excitation, without using enormous amounts of average power.

Many lasers are now available that can produce ultrashort pulses at high repetition rates. Titanium-sapphire lasers, for instance, are capable of producing ~100 fsec pulses over a broad tunable wavelength range (690 nm-1064 nm) with a high repetition rate, ~80 MHz. Similarly, solid state, doubled neodymium doped yttrium lithium fluoride (Nd: YLF) lasers, emitting 1047 nm, 175 femtosecond pulses at 120 MHz have also be used for multiphoton excitation.

Ti: Sapphire lasers are probably the most popular lasers because of the wavelength range that is available. These lasers can operate in both a continuous wave (CW) mode or in a mode that emits pulsed light. Lasers operating in this latter mode are said to be mode-locked (ML), which refers to the fact that the laser is locking in different frequencies together to form a pulse of a particular bandwidth.

The use of ultrafast mode-locked lasers for multiphoton excitation requires to consider several additional factors which are not necessary for continuous-wave lasers used for single-photon excitation. The length of the laser pulse (referred to as the pulse length or pulse width) ( $\tau$ ), the peak intensity produced at the focal plane ( $I_{\text{peak}}$ ), the average power of the laser at the specimen ( $P_{\text{avg}}$ ), the cross-sectional area of the beam ( $A$ ), and the pulse frequency ( $F_p$ ) or repetition rate are all important factors for achieving and maintaining efficient multiphoton excitation in the sample.

Raising the average power of the laser,  $P_{\text{avg}}$  (controlled by the Acousto-Optic-Modulator, AOM), will raise the peak intensity. However, raising the average power will also increase the amount of heat generated in the sample, which may damage vital processes or disrupt cellular structures.

The pulse frequency,  $F_p$ , is determined by the design of the laser and is not easily manipulated. For the Coherent Mira 900 Ti: Sapphire laser,  $F_p$  is equal to ~76 MHz.

The cross-sectional area of the beam,  $A$ , is an important term to consider when dealing with light focused through an objective. Simply put, reducing the cross-sectional area of the beam, for instance by focusing the beam through an objective, increases the intensity at the point of focus or in other words increases the amount of photons per area as we saw above.

The exact dimensions of  $A$  will vary greatly depending on the properties of the objective. In general, higher magnification, higher NA objectives will reduce  $A$ , similar to the way such objectives increase resolution. However, other considerations such as the transmission efficiency of the objective and the amount of dispersion produced by the objectives must also be considered as this will reduce  $P_{\text{avg}}$  or increase respectively. In addition, spherical aberration caused by the objective and sample and the diameter of the beam at the back aperture of the objective can also affect  $A$ . Thus, empirical determination of the best objective is often relied upon. (see Section 8.3.4 Objectives recommended for multiphoton excitation).

The pulse length,  $\tau$ , is a measure of the duration (length) of the pulse of photons being delivered to the sample, measured at the full width, half maximum. Increasing the pulse length, decreases  $I_{\text{peak}}$ . As mentioned above, ultrafast lasers are able to supply short pulses with a high duty cycle. Unfortunately, the pulse length is very difficult to measure, especially through a microscope objective. However, it is possible to make such measurements and users should refer to Wolleschensky et al. (1998) for details. The LSM 510 NLO fiber-delivery system contains a pre-chirping unit that is used to compensate for Group Velocity Dispersion (GVD) along the optical path. This system is capable of producing 120-200 fsec pulses at the sample, but the fiber imposes considerable restrictions on the peak power, the available wavelength range and the ease of tunability. Several factors that effect the pulse length are discussed below.

### 8.2.5 Optimizing the Peak Intensity without Frying the Samples

Although raising the average overall power is the easiest way to increase the peak intensity, excessive heat can destroy both live and fixed samples, as well as produce unwanted imaging artifacts. Assuming that one is using a laser with a fixed pulse frequency and a high magnification, high NA objective optimized for multiphoton microscopy (see Section 8.3.4 Objectives recommended for multiphoton excitation), the pulse length becomes the most important term to minimize.

The Spectral Bandwidth refers to the spectral frequencies of the pulse. Each short pulse produced by the laser has a broad spectral band centered around the selected wavelength. Spectral bandwidth and pulse length are inversely related. The wider the bandwidth, the shorter the pulse.

The Coherent Mira 900F produces pulses ranging from 70-150 fsec with a bandwidth range from 6-13 nm.

GVD is a temporal broadening of the pulse length as the pulse travels through normal dispersive media such as glass (see Diels and Rudolph, 1994 for more discussion). The pulse length becomes broader in dispersive media because the red shifted frequency components, with respect to the center wavelength, travel faster than the blue shifted frequency components. Pulses with a broader spectral bandwidth are more susceptible to the effects of GVD, as there is a greater difference in wavelength, and thus, velocities within the pulse (Fig. 8-3). In addition, the amount of dispersion is related to the thickness of the dispersive media (see Wolleschensky et al. 2001 for review). When possible, thinner glass optics and lenses are used along the routing path.

Within the laser, a prism pair is used to adjust the spectral bandwidth of the laser pulses. However, outside the laser, glass elements within the microscope and scan module, within the objective, and along the routing path, can lengthen the pulse. In this case, the broader the spectral bandwidth, the more broadening of the pulses will be caused by GVD. Thus, for direct-coupled systems without the use of a prechirping unit, it is advantageous to adjust the laser so that the bandwidth of the pulse is at a minimum. For instance, if the bandwidth is less than 7 nm, the pulse length at the sample will be approximately 300 fsec. If the bandwidth is 12 nm, the pulse becomes substantially broadened by the same dispersive elements so that the pulse length is about 700 fsec at the specimen.

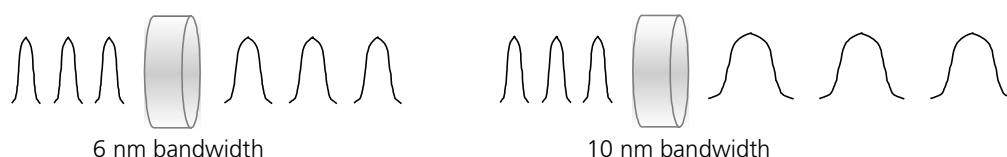


**Fig. 8-3 Effect of GVD on short pulses with a broad bandwidth. The broader the bandwidth, the more the pulse is stretched. Longer wavelengths travel faster through the glass than shorter wavelengths in the pulse. Thus, a positively chirped pulse is broadened.**

It is possible to compensate for GVD along the routing path and in the microscope to preserve the pulse length to the sample. By using a pulse stretcher/fiber combination, as is the case with the LSM 510 NLO GDC fiber delivery system, a pulse length of 120-200 fsec can be preserved at the sample (see Wolleschensky et al., 2001).

This system consists of a 5 W Verdi/Mira 900F laser system, a Grating Dispersion Compensator (GDC), a 3 meter single-mode fiber and a Post-fiber compressor unit (PFC). In this system, 100-150 fsec ( $10^{-12}$  nm) pulses exit the laser and enter the GDC. The grating compensator within this unit applies a negative chirp to the pulses and stretches the pulses to 6 psec. As the pulses pass through the 3 meter fiber, the 6 psec pulse becomes compressed due to GVD within the fiber and exits the fiber as a 3 psec pulse. Seven passes through the post-fiber compressor, which contains additional dispersive media, further compress the pulses as they enter the microscope so that at the sample, the pulses are now back to being chirp free at a pulse length of about 120 fsec.

This system enables the user to achieve efficient excitation of the fluorochrome with minimal power, by minimizing the pulse length and maximizing the peak intensity using low average power. Although effective at preserving the pulse length, this system has several limitations. First, due to self phase modulation, the fiber has an upper limit for the deliverable peak power (5.5 kW for a 120 fs pulse at a repetition rate of 76 MHz and at an average power of 50 mW). In a direct-coupled system the full power of the laser (~750 mW) can be sent to the sample resulting in peak powers greater than 80 kW, although this is rarely needed. Second, the fiber has a wavelength range of 750-950 nm for a 10 W pump laser and 750-900 nm for a 5 W pump laser. This limits the available wavelength range of the laser which is 680-1000 nm. Third, the laser can be difficult to align through the pulse stretcher, especially for novice users. Despite these limitations, this system provides an ideal imaging configuration for users who are concerned about keeping the average power low while imaging or placing the scan module on different microscope stands.

### 8.3 Using the LSM 510 NLO direct coupled system: Practical considerations for optimal imaging

#### 8.3.1 Coupling the Coherent Mira 900F to the LSM 510 NLO

Coupling an ultrafast laser to a laser scanning microscope is a fairly simple matter, if several key considerations are understood. Typically, the routing kit for coupling the LSM 510 NLO to the Coherent Mira 900F will consist of the following components: a beamsplitter optic, used to send a small percentage of laser output to a Rees Analyzer; an Acousto-Optic Modulator (AOM), used to control the intensity of the beam and for beam blanking (allowing for region of interest (ROI) and bi-directional scanning and for performing Auto-Z-Brightness correction); two 45° mirrors for directing the beam to the microscope on the table; and a 1 meter lens. In the case of an upright system, the beam is brought up into the scan head via a periscope, whereas for an inverted microscope, the height of the beam will be adjusted by a smaller periscope positioned in place of the second turning mirror. These devices ensure that the beam remains parallel to the table when horizontal and enters the scan head at the proper height (see diagram). The 45° routing or turning mirrors are adjustable and will be used routinely to peak the coupling of the beam into the scan head. The 1 m lens is used to expand the beam to fill the back aperture of the objective. It is mounted in a fixed position by a trained service engineer during installation and should not be adjusted by the user (Fig. 8-4).

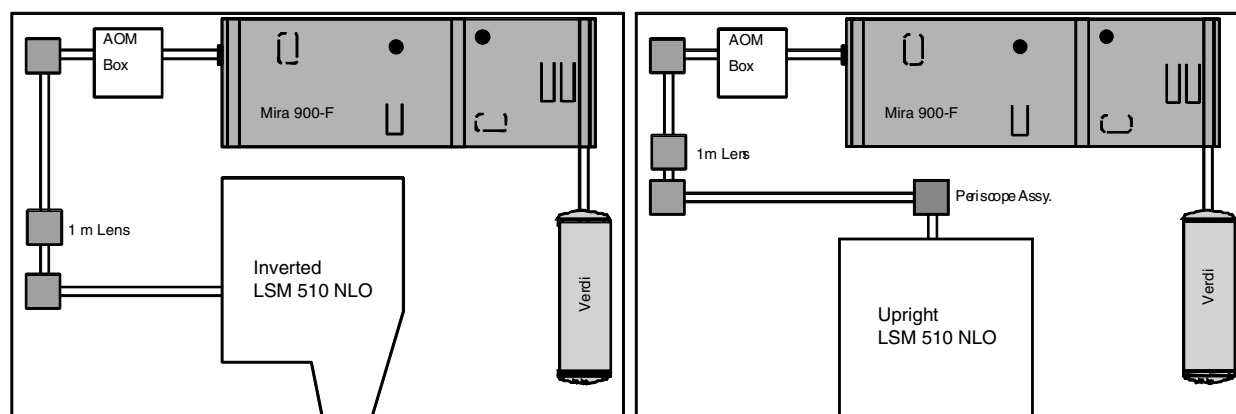


**Fig. 8-4** Typical alignment scheme for the LSM 510 NLO direct-coupled system using an inverted (left) or upright (right) microscope.

#### 8.3.2 Using and tuning the Coherent Mira 900F – A simplified protocol for direct-coupled LSM 510 NLO systems

We have developed a simplified tuning protocol for the Coherent Mira 900F in order to preserve alignment of the beam into the scan head while tuning. This protocol will cover tuning over most of the usable wavelength range of the Mira (~720-950 nm), but slight adjustments in the alignment may be necessary for tuning the complete range (~700-990 nm).

### 8.3.2.1 Turn on procedure

Turn on the system by switching the key on the Verdi Controller Box from STANDBY to ON. Turn on the TEC chiller that cools the Verdi baseplate and Ti: Sapphire crystal. Allow the system at least 30 minutes to warm up. The laser should be left in the standby position, unless the laser will not be used for a very long period of time (> 2 weeks). If the laser is completely shut down, the system will require at least an hour to warm up. Turn on the Mira 900F controller box using the switch on the back panel. Turn on the IST-Rees Spectrum Analyzer and oscilloscope.

 Tuning and mode-lock can be achieved without a Rees Analyzer, however it is recommended that this is included on all systems in order to adjust the bandwidth of the pulse accurately and in order to adjust the AOM frequency to match the output wavelength.

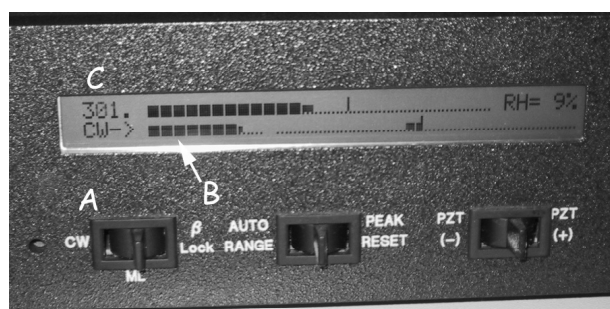


**Fig. 8-5** The Mira Controller display panel. (A): CW-ML-β lock switch to initiate mode-lock. (B): Indicator for CW break-through. In CW mode, the range would be full, whereas for a laser in mode-lock, the range would be empty. The laser here is partially mode-locked with CW breakthrough as in Fig. 8-7/B. (C): The power indicator from the Optima system in arbitrary units.

After the laser has warmed up, switch the CW-ML-β lock switch to the ML position (Fig. 8-5/A). Make sure that the Rees

Analyzer is adjusted so that the center wavelength is visible on the oscilloscope screen (a blinking reference marker should be seen) by adjusting the up and down buttons (indicated by arrows) on the Rees Analyzer control box (Fig. 8-6).

A bell-shaped curve should appear at the center wavelength, indicating good mode-locked operation (Fig. 8-6, Fig. 8-7/A). If the laser is partially mode-locked, but has some CW break through exiting the cavity, a spike will appear along with the curve (Fig. 8-7/B). If the laser is not mode-locked at all, a sharp spike will be seen (Fig. 8-7/C).

A bell-shaped curve that has a broad noisy line, as in Fig. 8-7/D, indicates that Q-switching is occurring.

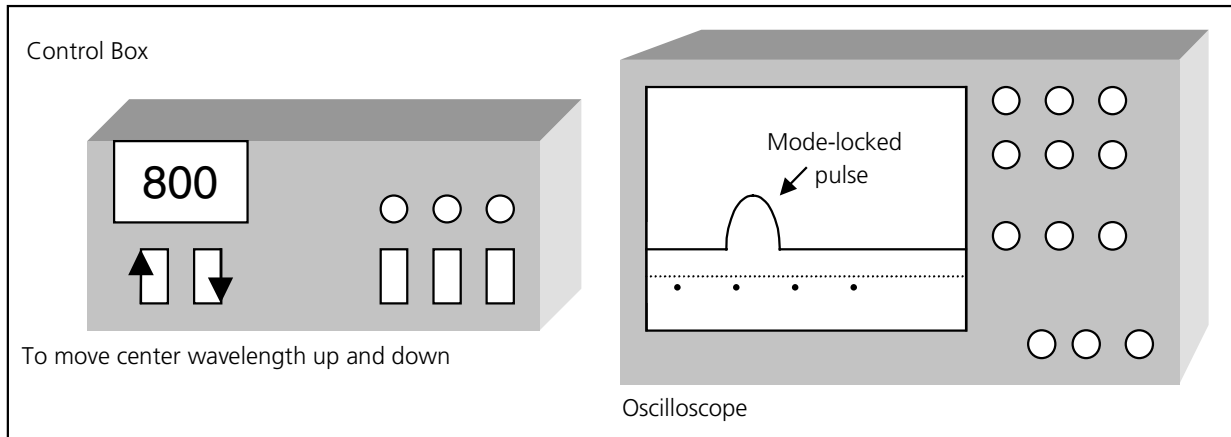


Fig. 8-6 Schematic of a IST Rees Spectrum Analyzer

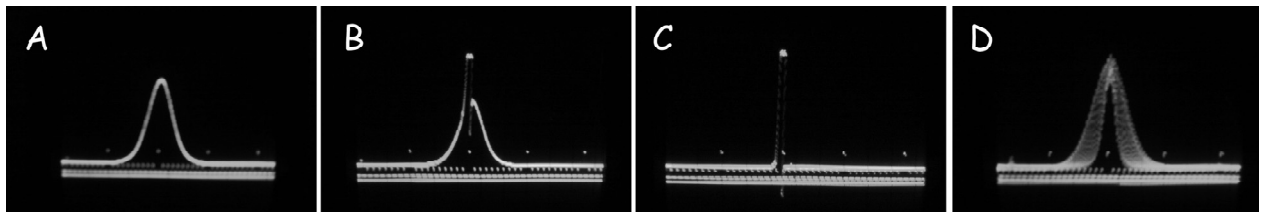
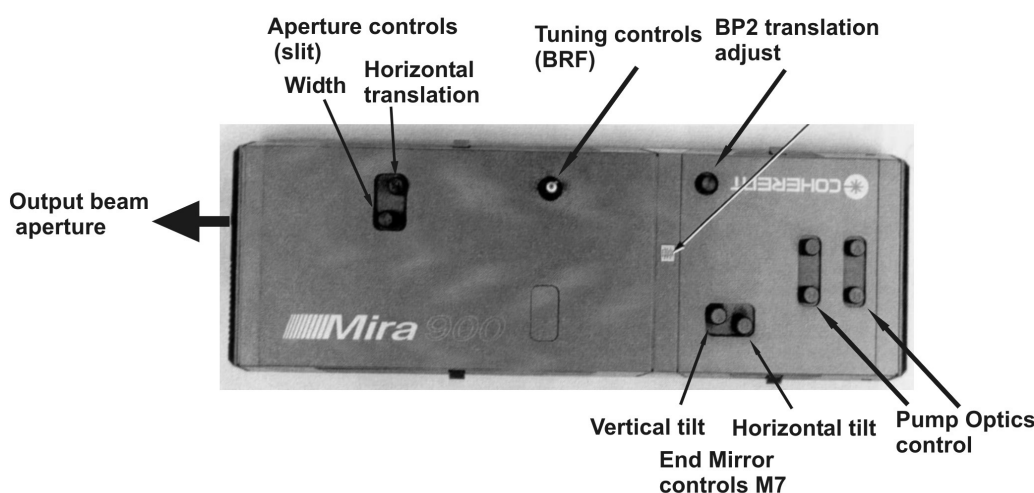


Fig. 8-7 Examples of common oscilloscope beam profiles for the Coherent Mira 900F. A, stable mode-locked operation. B, partially mode-locked operation with CW breakthrough. C, pure CW operation indicating no mode-lock. D, Q-switching indicating that the slit aperture is too small to reinforce stable mode-lock.

### 8.3.2.2 Achieving stable mode-lock

If a stable, mode-locked pulse does not appear at start-up (Fig. 8-7/**B-D**), adjustments should be made to stabilize mode-lock. Every attempt should be made to establish a stable mode-lock at system start up and shut down, and mode-lock should always be established before tuning. This will help preserve the alignment of the laser. Simple adjustments in the slit width may correct the problems seen in Fig. 8-7/**B** or Fig. 8-7/**D**. CW breakthrough often results when the slit opening is too large. Try closing the slit slightly. This can also be adjusted by turning BP2 in the counter-clockwise direction, but adjustments in the slit width should be made first. Q-switching often results when the slit width is too small, so opening the slit slightly should eliminate this problem. When imaging, CW breakthrough will lead to gaps in the image since the laser is going in and out of mode-lock while the scanner is in motion, whereas Q-switching can lead to wavy lines being formed in the image due to power fluctuations (see Fig. 8-8 for description of the Mira controls).

If a mode-locked pulse is not evident after start-up, be sure that the laser has had ample time to warm up. If pure CW operation is seen (Fig. 8-7/**C**), adjustments in laser alignment will need to be made. First make SMALL adjustments up and down with the BRF micrometer. Often a mode-locked beam profile will appear. Then you can stabilize the beam at this wavelength and make small adjustments in the alignment to center the beam at the wavelength of interest (see below: Tuning the MIRA 900F to a new wavelength). If a bell-shaped curve does not appear, try opening and closing the slit a quarter rotation. Next, make small adjustments in BP2, both in the clockwise and counterclockwise direction.



**Fig. 8-8 Mira 900F controls**

If all adjustments fail and a mode-locked beam cannot be found, set the BRF to the desired wavelength by locating the CW spike on the oscilloscope (Fig. 8-7/**C**). Next, open the slit to allow maximum power through to the output coupler. Then rotate BP2 to allow less glass in the path and until the laser stops lasing. (The Optima power reading on the Mira will be reduced to the baseline, Fig. 8-5/**C**). Note the position of the mark on the BP2 knob and then rotate the knob back to add glass four full rotations. Close the slit until a mode-locked beam profile appears. Maximize the power by making very small adjustments with the M7 mirror (usually only horizontal adjustments are necessary).

Re-adjust the opening of the slit apparatus to ensure stable mode-lock. At this point, since the slit width has been fully opened and then closed again, it may be necessary to make SMALL adjustments in the horizontal position of the slit. While monitoring the power level reading on the MIRA output controller, slide the slit translation knob back and forth to find the optimum position for the slit. The optimum position will result in a higher power reading. Re-adjust the slit width to achieve stable mode-lock.



**CAUTION:** This horizontal position of the slit should only be adjusted after the slit has been opened completely to re-tune the laser and only small adjustments should be necessary. Large adjustments in the position of the slit indicate that the alignment of the laser is not optimal and, as a result, the laser may not be aligned into the AOM. Realignment of the laser and the AOM will require the help of trained service engineers.

### 8.3.2.3 Tuning the MIRA 900F to a new wavelength

Once a mode-locked beam profile is stabilized, one can easily tune to a new wavelength. To do this, turn the BRF in the direction required to move to the desired wavelength. You will see the curve on the oscilloscope move. The shape of the curve may begin to change. The bell-shaped curve may begin to get flatter or taller, or spikes may appear in the curve (Fig. 8-7/**B**), or the single line of the trace may begin to look wavy (Fig. 8-7/**D**). Adjusting the slit width and/or BP2 will restore stable mode-lock as indicated above. It is recommended that you make small adjustments in the wavelength using the BRF and then optimize the mode-lock and then to repeat this process until you have arrived at the desired wavelength.

Once the beam profile is centered over the desired wavelength, again optimize mode-lock by adjusting BP2 and the slit width. Small changes in M7 may help to recover more power and produce a more stable mode-locked beam. In some cases, maximum power output will only be achieved if small adjustments in the fine-tuning controls for the pump laser are made (rear-most pump optics control knobs). Balance changes in the rear pump optics with M7.



**DO NOT MAKE ANY ADJUSTMENTS IN THE COURSE ALIGNMENT OF THE PUMP BEAM USING THE FORWARD PUMP OPTICS CONTROL KNOBS.**

### 8.3.2.4 Adjusting the bandwidth of the pulse

For direct-coupled systems using no pre-chirping unit the bandwidth of the pulse should be minimized to limit the effect of GVD along the routing path and through the microscope and the objective. Therefore, the final adjustment to the mode-locked beam should be to lower the bandwidth of the pulse as much as possible by adjusting BP2 (usually removing glass) and opening the slit. Fig. 8-9 shows an actual trace from the oscilloscope of a direct-coupled system. The pulse is mode-locked and centered at 800 nm. To estimate the bandwidth, the full-width, half-maximum (FWHM) is used. For this trace the bandwidth appears to be approximately 6 nm, which is ideal for imaging with a direct-coupled system.

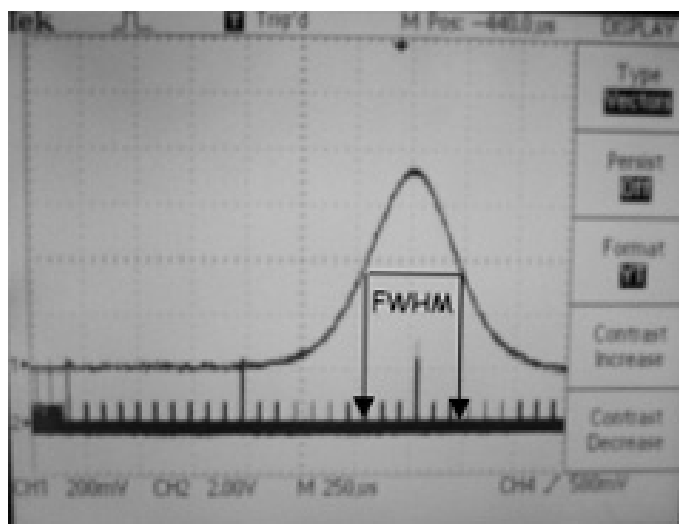


**Fig. 8-9** The beam profile of a mode-locked laser output. The bandwidth of the pulse is the full width at half maximum (FWHM) of the bell shaped curve. In this case the bandwidth is approximately 6 nm, which is ideal for direct-coupled systems.

### 8.3.3 Alignment of the Coherent MIRA 900F into the LSM 510 NLO scan head

The alignment of the laser through the AOM and into the scan head is critical for producing high quality images using multiphoton excitation. Below are two protocols that can be used to optimize alignment of the beam into the scan head.

#### 8.3.3.1 Quick alignment protocol

After the system is installed and aligned by a qualified service engineer, it is often the case that only small alignment adjustments are necessary. For instance, proper alignment should be verified after the laser is tuned to a new wavelength. Below is a quick and easy protocol that can be used to center the beam into the back aperture of the objective lens for optimum image quality.

Confirm that the correct wavelength for the laser is set in the laser control panel in the software. The wavelength can be changed by selecting the modify option. Refer to the Rees analyzer or the BRF setting to determine the wavelength of the MIRA 900F.

Start by scanning a sample that is normally excited by the wavelength of the external laser. For instance, a pollen grain slide (Carolina Biological) or a Fluocells sample (Molecular Probes) can be used. (NOTE: This procedure may cause bleaching of the sample.)

Adjust the laser power and gain so that the sample is visible in the image acquisition window.

Scan the sample using the fast XY scanning mode.

Using the signal intensity as a guide, peak the alignment of the beam. Begin by using the alignment mirror closest to the laser (first turning mirror). Make improvements using both alignment pins on the mirror mount. (NOTE: a small hex wrench (Allen key) may be needed to adjust alignment). When the best signal intensity is obtained by tweaking the mirror closest to the laser, now make improvements by tweaking the mirror closest to the microscope scan head. Go back and forth between these mirrors to walk the center the beam onto the back aperture of the lens.

After alignment, it may be necessary to optimize the AOM (Acousto-Optic Modulator) frequency, if an AOM is used. Open the modify window in the laser control panel. Confirm that the correct wavelength is set for the wavelength of the external laser. With the sample in place and while scanning in the Fast XY mode, slide the AOM frequency slider to the right and left to obtain the brightest signal. A peak should be found within the range of the slider. If not, the beam may be misaligned through the AOM. If this is the case, contact a qualified service engineer. NOTE: Confirm alignment of the beam into the scan head using the above protocol before modifying the AOM frequency.

As a final verification of proper alignment, check the alignment of the beam onto the back aperture directly by viewing the projected beam without the objective in place. To do this, place a white card on the stage (Fig. 8-10/A) or lens paper on the specimen holder for an inverted microscope.

Remove one objective, select 50-100 % transmission, HFT KP 680 or 700, and Fast XY scan. When the system is scanning, a round, red spot should appear on the card (Fig. 8-10/B). Seeing this beam may be aided by using an IR viewer, especially at longer wavelengths.

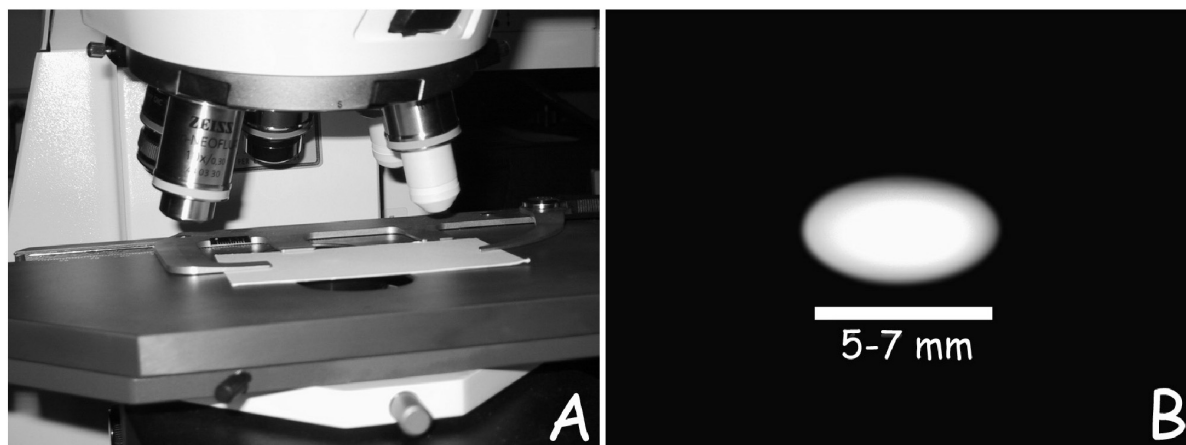


**Fig. 8-10 (A) Setup for checking the beam alignment; (B) Optimal shape of the NIR laser spot**

Ideally this spot should be 5-7 mm in diameter and should be completely round and uniform. If the beam appears to be clipped (flat on one side), small adjustments in the routing mirrors can improve the alignment (see above). Shadows in the illuminated spot may indicate dust or debris on the routing optics or in the scan head (check all visible elements for debris, then contact a service engineer if the problem persists).

If proper alignment cannot be established using this protocol or if the image quality appears to be poor, use the advanced alignment protocol to peak alignment.

### 8.3.3.2 Advanced alignment protocol

When the system is installed, the service engineer will establish alignment of the laser beam into the scan head by verifying the overlay between the NIR laser and one of the VIS lasers. Although routine use usually does not usually require a complete realignment with the scan head, tuning the laser over large wavelength increments or changing or cleaning the optics in the laser can cause gross changes in beam pointing. If this occurs, it is best to use the following protocol to re-establish proper alignment with the scan head. For this protocol, a partially reflective grid slide is needed (Part number 474028-0000-000, Test Grid Specimen for LSM). Care must be taken to use low amounts of laser power when using this slide or the grid can be easily burned.

Begin by confirming that the correct wavelength for the laser is set in the laser control panel in the software. The wavelength can be changed by selecting the modify option. Refer to the Rees analyzer or the BRF setting to determine the wavelength of the MIRA 900F.

Next, place the partially reflective grid slide on the microscope stage. Bring the grid slide in focus using the 10x Plan-Neofluar objective and transmitted light. Configure the scan head as follows (Fig. 8-11):

This configuration is designed to use the PMTs to detect the reflection of the NIR and VIS laser light off of the grid slide so an image of the grid is made on the screen. For this protocol, the 543 nm line has been chosen. The HFT KP 700/488 beam splitter is used to avoid sending too much 543 nm laser light to the reflective slide. A KP 700/543 beam splitter can be used, but care must be taken not to burn the slide. Alignment using this procedure will ensure that the NIR and VIS lasers overlay on the combining mirror when they enter the scan head.

To perform the alignment, set the laser power for both lasers at 3 % (1 % for a MIRA 900F with a 10W pump laser) and adjust only the gain to improve the intensity of the signal.



**WARNING:** Too much laser power can cause damage to the grid slide! Be sure attenuation is set before scanning.

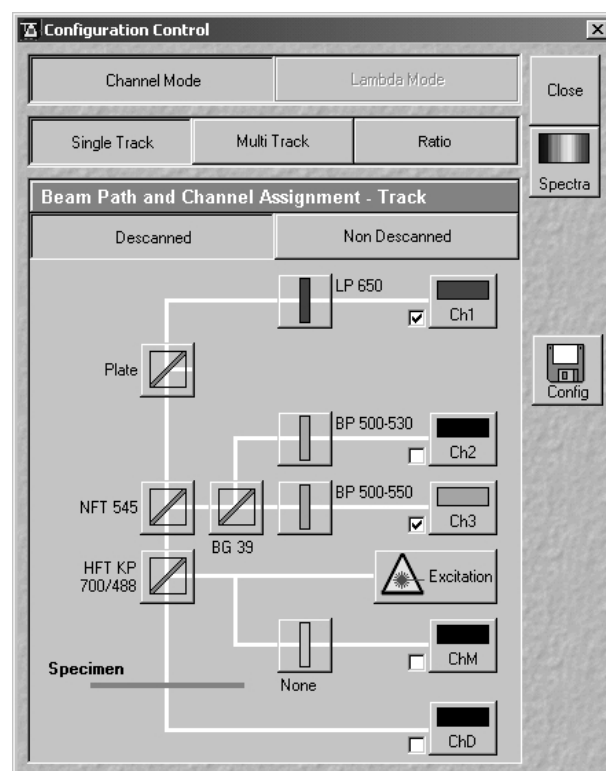


**Fig. 8-11** Configuration for testing the overlay of the grid reflection images gained with the vis (543 nm) laser and the NIR laser

Begin scanning using the FAST XY mode. An image of the grid should appear on the screen. If not, adjust the gain for each channel so that the output from both channels is visible. The two colors represent the reflection of the 543 nm line (green) and the reflection of the NIR laser (red) on the metallic grid surface. The focus may also need to be adjusted in order to get the optimal output from both channels. If the red image is out-of-focus when the green image is in focus, the collimating lens should be adjusted so that both beams are focused on the same spot. To adjust the collimator, open the Maintain panel in the LSM 510 software. While the laser is scanning, click on the pinhole button. At the bottom of this panel, there is a slider to adjust the NIR collimator.

 DO NOT ADJUST THE VIS COLLIMATOR.

Adjustments in the NIR collimator should improve the focus of the NIR beam. If no signal at all is detected in the red channel, turn up the laser transmission in small increments and begin peaking alignment.

 Note that once alignment is improved, the laser intensity will need to be attenuated to avoid burning the slide. If no red signal at all can be found, contact a service engineer.

Once both beams are in focus, begin optimizing the overlay of the grids by first adjusting the routing mirror that is closest to the laser. Make small adjustments using both alignment screws while watching the effect on the monitor screen. Adjustments of this mirror will increase the intensity of the red signal. Readjust the gain as needed. After optimizing the alignment using this mirror, begin adjusting the mirror that is closest to the scan head (NOTE: A small hex wrench [Allen key] may be needed to adjust alignment). Adjustments in this mirror will improve the alignment of the NIR overlay on the VIS overlay. Go back and forth between these mirrors to walk the center the beam onto the back aperture of the lens.

### 8.3.3.3 Tips on maintaining alignment with the scan head

Since the NIR beam is aligned into the scan head through mirrors and free space, it is possible that any alteration in these routing components can effect proper alignment. Below are some tips to maintaining good alignment:

- Use the simplified tuning protocol in Section 8.3.2.3 to tune to different wavelengths
- Do not move the position of the 1m lens or the beamsplitter used to send the signal to the Rees analyzer. Even small adjustments of these components may cause significant changes in the alignment of the routing optics.
- If the laser is cleaned or optics within the cavity are changed, note the position of the output of the beam before adjustments are made and realign the beam to this position when the laser is optimized. An aperture stand supplied with the laser is useful for this.
- If recurring alignment drifts or power fluctuations in the laser are observed, consider floating the optical table and/or regulating the room temperature more closely. Changes in the temperature of the table or optical components can often cause drift in alignment of the laser and routing optics.
- Avoid tuning the laser in increments larger than 50 nm without peaking the alignment.

### 8.3.4 Objectives recommended for Multiphoton Excitation

For nonlinear microscopy, objectives should be optimized for the following parameters: high transmission in the NIR and the VIS-wavelength range, long working distance with a high numerical aperture, limited pulse broadening due to GVD, a uniform GVD across the pupil of the objective for the excitation wavelength range and a small propagation time difference (PTD). As we have already discussed, low transmission in the NIR can lower the average power at the sample, thus lowering the peak intensity.

Long working distance objectives with a high numerical aperture are clearly favored for deep imaging so that the beam can be focused deep into the tissue and the emission photons can be collected efficiently. Objectives should have limited GVD to reduce the chance that short pulses will be lengthened en route to the sample, which will again reduce the peak intensity.

In addition to GVD, chromatic aberration of objectives leads to pulse distortions. Specifically a radius-dependent group delay is introduced (Kempe et al., 1993; Netz et al., 2000). Therefore, different radial portions of the beam across the pupil of the objective arrive at different times at the focal region and cause a temporal broadening of the pulse. This results in lower peak intensity in the focal region (Fig. 8-12). This effect is also referred to as PTD.

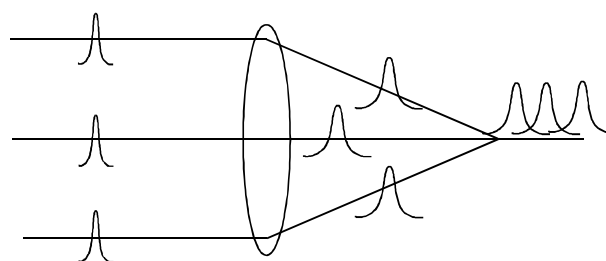


**Fig. 8-12 Schematic pulse transformation by a singlet lens showing the influence of chromatic aberrations on the peak intensity due to Propagation Time Difference (PTD).**

Table 1 summarizes the important characteristic parameters for objectives recommended for nonlinear microscopy and for the optics inside the LSM 510 NLO including the microscope stand. The dispersion parameters were calculated based on the material data and the thickness of each optical element on axis. For comparison, the dispersion parameter for the optics within the LSM 510 NLO including the microscope stand and the AOM is 7500 fsec<sup>2</sup>.

The variation of the dispersion parameter for different beams across the pupil of the objective is listed in the fourth column. It can be seen from both parameters that the pulse broadening is nearly independent of the particular objective used and the position of the beam across the pupil of the objective. The pulse broadening due to the GVD of the different objectives and the LSM 510 NLO including the microscope stand and the AOM was calculated for 100 fs pulses at a wavelength of 800 nm and is listed in column 5.

The pulse broadening due to PTD is listed in the last column. The PTD was calculated for the whole optical setup, since it depends on the chromatic aberrations of the complete system including the LSM 510 NLO and the microscope stand for a wavelength of 800 nm. The PTD effect is negligible if the pulse length is not much shorter than 100 fsec. It can be seen that the special IR corrected objectives show a smaller PTD in comparison to the standard UV/VIS corrected objectives.

Objective	Working Distance [mm]	Dispersion Parameter [fsec] <sup>2</sup>		Pulse broadening factor of 100 fsec pulse	Max. PTD [fsec] (*)
		On axis	Variation		
IR-Achroplan 40x/0.8 W	3.61	1714	± 20	1.14	-3
IR-Achroplan 63x/0.9 W	2.00	1494	± 15	1.11	-9
Plan Neofluar 40x/1.3 oil	0.20	2328	± 30	1.23	9
Plan Apochromat 20x/0.75	0.61	1531	± 10	1.12	10

**Table 1 Summary of specific parameters for objectives recommended for 2-Photon applications. All data were measured at 800 nm. (\*) Propagation time difference (PTD) is calculated for the whole optical setup including the LSM 510 NLO and the microscope stand.**

Negative values indicate that pulses at the edge of the pupil are delayed with respect to pulses traveling on axis.

With regard to transmission, objectives for biomedical applications traditionally have been optimized for UV and visible range imaging. Thus, many are not corrected for transmission of NIR or IR light. The transmission of an objective depends strongly on the design of the antireflection coating. Typical transmission curves for two different objectives are shown below. The Achroplan series is coated with UV/VIS-antireflection coating giving optimal performance from 350 nm to approximately 800 nm. In contrast, the IR-Achroplan series has a VIS/IR coating that enables high transmission from 420 nm to 1400 nm. The Achroplan objectives are best for multiphoton applications, where excitation is below 850 nm and the fluorescence from the specimen is in the ultraviolet or lower visible wavelength range.

These criteria describe the imaging parameters for many ion indicators, nuclear dyes such as DAPI or Hoechst, Blue Fluorescent Protein, and Fluorescein or Alexa 488. The IR-Achroplan objectives are best for multiphoton applications requiring an excitation wavelength greater than 850 nm and where the fluorescence emission is above 420 nm (Fig. 8-13). These latter criteria apply to many dyes, such as Dil, and many of the fluorescent proteins, such as CFP, GFP, YFP, and dsRed. However, some important fluorochromes can be imaged well with either objectives.

Rhodamine, for example, has a multiphoton absorption peak at 840 nm, and like Alexa 568 it can be excited well at 800 nm. Thus, the examples are given to indicate ideal imaging criteria; however, non-optimized parameters can often be used to produce high-quality images.

While the Achroplan objectives clearly provide the best transmission curves with the longest working distance, other objectives have proven to be useful for multiphoton imaging. For instance, the Plan-Apochromat objectives have favorable properties for multiphoton imaging as Table 1 indicates. In addition, the C-Apochromat 40x W/NA 1.2 and its 63x counterpart have proven to be very effective objectives, perhaps due to their high NA and collection efficiency. Moreover, these objectives have a 0.23 and 0.25 mm working distance, respectively, and can be very useful for collecting large 3-D data sets. Unfortunately, these objectives begin to decline in transmission at around 840 nm, so they are not optimal for dyes with more red-shifted excitation wavelength absorption maxima, but can often be used without concern for the lost photons

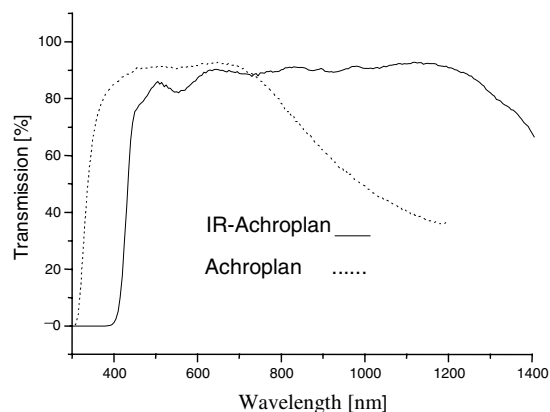


**Fig. 8-13** Typical transmission curves of an IR-Achroplan and an Achroplan.

### 8.3.5 Choosing Fluorescent Probes for MPLSM

Presently, there are thousands of different fluorochrome derivatives and conjugates that can be used to study a variety of biological events. Many of these fluorochromes have been optimized for single-photon excitation and scientists are just beginning to concentrate on developing optimized fluorochromes for multiphoton imaging applications (see Albota et al, 1999). Furthermore, it is difficult to predict whether or not a particular dye will be useful for multiphoton imaging and many of us have relied on trial and error while a greater understanding of the physical principles of multiphoton excitation is evolving. That being said, there are some important parameters that one can use to help predict which dyes may be best for a particular application.

Similar to the way one would choose a fluorescent probe for conventional fluorescence microscopy, the best fluorochromes for multiphoton imaging are the ones that efficiently absorb light, reliably emit fluorescence, and are photostable. Values such as the multiphoton cross-section and the fluorescence quantum yield are important to consider when choosing a fluorochrome.

The multiphoton cross-section is a measure of how strongly a fluorochrome absorbs photons at a given wavelength and is expressed in units of  $10^{-50}$  cm<sup>4</sup> sec/photon or 1 GM (Goeppert-Mayer unit, after the scientist who first predicted multiphoton absorption, Maria Goeppert-Mayer). A list of cross-sections can be found in Xu (2000) or at

[www.uga.edu/caur/dyechart.pdf](http://www.uga.edu/caur/dyechart.pdf)

The web-site shows a collection of excitation cross sections for various dyes. Currently available dyes have multiphoton cross-section values ranging from 40-200 GM (see Xu, 2000).

These values are only an indication of how well a dye will perform in biological imaging using MPLSM. A one to one correlation between the cross-section and dye performance cannot always be drawn. Measurements of multiphoton cross-section are usually performed with the dye dissolved in organic solvents or at non-physiological conditions and the local environment of a dye may influence absorption and emission characteristics. Also, these values are determined at an optimal pulse-width that cannot always be achieved at the level of the specimen. Although the cross-section is a valuable first approximation of how a dye will perform, trial and error provides the truest test for a particular application.

The multiphoton cross-section not only provides information about how well a particular molecule is excited by pulsed NIR light but also indicates the multiphoton absorption peak, a value that has been surprisingly difficult to predict. While it may seem logical that the two-photon absorption peak should be twice the one-photon peak, this has not proven to be the case. An emerging rule of thumb is that the peak is usually shorter (more blue-shifted) than twice the one-photon absorbance peak (Xu, 2000). However, one should also keep in mind that the brightest signal may not be obtained at the predicted excitation peak but at the point where the excitation peak and the power peak of the laser overlap.

For tunable Ti: Sapphire lasers, there is a peak output at or near 800 nm, with less average power produced at lower and higher wavelengths; as a result, it is possible to excite a given dye at a non-optimal wavelength by using more power. However, more power may also mean more heat or bleaching, so one should be careful to optimize the signal-to-power ratio.

Blue/Cyan dyes

Alexa 350 (780 nm-800 nm)  
Hoechst (780 nm-800 nm or 900-1100 nm)  
DAPI (780-800 nm or 900 nm-1100 nm)  
CFP (800 nm-900 nm)

Green dyes

Oregon Green (800 nm-860 nm)  
Alexa 488 (800 nm-830 nm)  
GFP (840 nm-900 nm)  
BODIPY (900-950 nm)  
FITC (750 nm-800 nm)  
DiO (780 nm-830 nm)

Yellow Dyes

YFP (890 nm-950 nm)

Orange dyes

DiA (800 nm-860 nm)

Red dyes

DiI (830-920 nm)  
Rhodamine B (800 nm-860 nm)  
Alexa 568 (780 nm-840 nm)

**Table 2 Recommended multiphoton excitation wavelengths for common dyes.**

In addition to how well a molecule absorbs light, the best molecules to choose are the ones that also efficiently release light as the molecule relaxes back to the ground state. The fluorescence quantum yield is a measure of the proportion of emission photons that are shed per excitation event.

In general, this value is the same for one- or multiphoton excitation and values for common fluorochromes can be found in Haugland (1996).

As mentioned above, photostability is an important factor when choosing a dye. Photobleaching is minimal in out-of-focus regions using MPLSM, but bleaching still occurs at the point of focus. In fact, some dyes that are relatively stable using one-photon excitation, have more rapid bleaching rates using MPLSM (Patterson and Piston, 2000). This phenomenon is not fully understood, so the bleaching rate of dyes of interest should be tested for each application. In cases where rapid bleaching occurs, we have found that ProLong (Molecular Probes, Eugene, OR) has helped stabilize the signal in fixed samples.

Table 2 is a rough guide of fluorochromes recommended by the Biological Imaging Center at Caltech. Currently, there is no comprehensive reference for all dyes excited by two- or three-photon excitation for the user to refer to for information on the peak absorbance wavelength or relative brightness of a given dye.

The information given below is based on empirical observation and does not reflect a serious, scientific investigation of all dyes, nor does it indicate the exact optimal excitation wavelength for each dye in question. Instead, this list is offered as a rough guideline of what is known to work for various imaging applications and the user is encouraged to empirically determine which dyes are most useful for their own applications. Clearly the success of any fluorescence imaging experiment relies on how well the target is labeled. The same is true for MPLSM.

### **8.3.6 Samples your mother should have warned you about**

While multiphoton excitation has many advantages, there are also some disadvantages to using high intensity NIR or IR light for fluorochrome excitation. Probably one of the biggest disadvantages is the heat that is generated via the absorption of NIR photons by water. The local heating that is caused can affect vital cellular processes, such as cell replication (König et al., 1996) and other growth abnormalities in sensitive specimens. Thus, great care should be taken to maximize PMT settings so that minimal power levels can be used while imaging. Particular care should be taken when imaging cells or specimens that contain molecules that absorb light such as melanin.

In some cases, the absorption of NIR photons can cause dramatic local heating effects and cause cells to explode. This effect has been seen frequently in zebrafish embryos, but can be avoided by blocking melanin production with chemical agents, such as PTU or by using albino embryos.

Other molecules, such as salt crystals, can also focus light within tissues and intensify heating effects. This can also lead to imaging artifacts, perhaps due to signal produced via second harmonic generation (SHG). In Fig. 8-14 Calcium Carbonate crystals in the inner ear of the frog have produced blotchy artifacts.

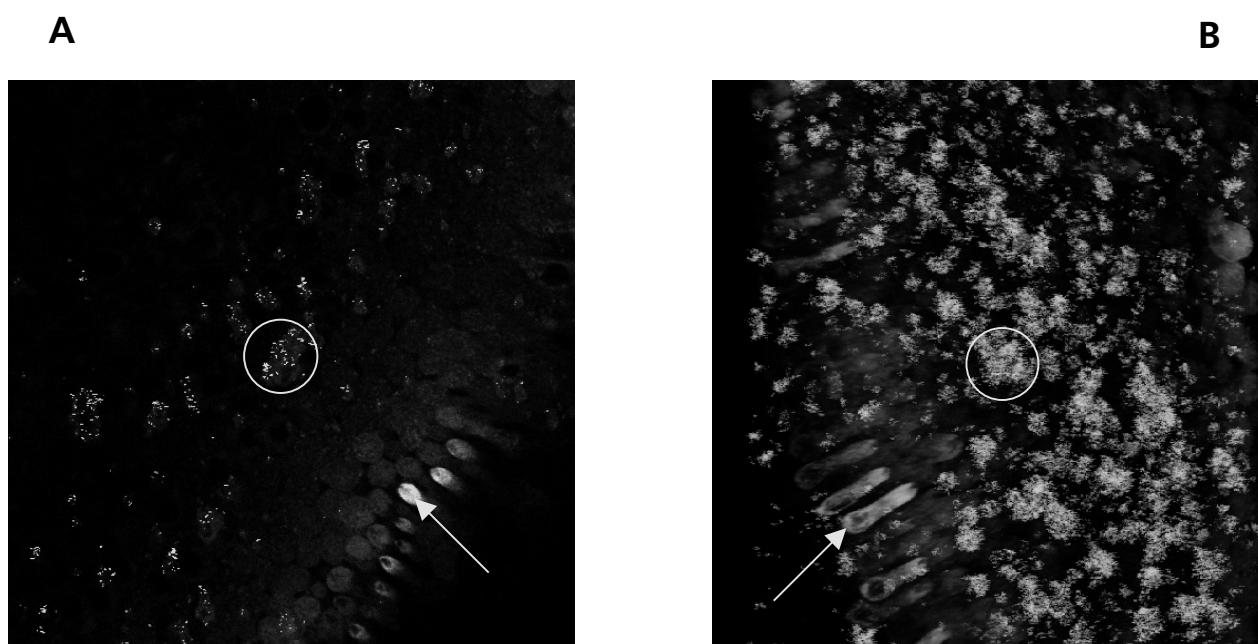


**Fig. 8-14** Multiphoton image (A) and stack of images (B) of the frog otolith. Cells have been fluorescently stained by soaking the freshly prepared specimen in FM164 (arrow). Signal produced by the artifact is shown inside the circle. Sample courtesy of Bill Roberts, University of Oregon.

The artifacts completely obscure the three-dimensional reconstruction shown in Fig. 8-13/B.

This effect is not specific to Calcium Carbonate and has been seen in other samples, such as those with crystals of salt from evaporated sea water (data not shown).

Artifacts can also occur in fixed tissue. Local heating effects can cause bubbles to form in the mounting media or induce localized photochemistry in some mounting medias. It is important to test all mounting medias before use for multiphoton imaging. Fig. 8-15 shows an image where a large artifact is produced in an image using multiphoton excitation. In this example, Epon-araldite resin, generally used for EM embedding, was used. This is particularly bad for multiphoton imaging as it quickly becomes heated using focused NIR light.

Similar effects can be seen if oil and water are mixed, such as on the top of a coverslip when different immersion objectives are used on the same sample. Similar to the way water sizzles in a frying pan, steam will be produced from the focused heating of the oil and image artifacts result. Usually, these types of artifacts are dynamic as the water evaporates or the oil breaks down and the artifact may grow as you image for a longer time. It is important to clean the coverslip of your samples well with ethanol to dry off the water before mounting in oil or to clean off the oil before mounting in water.

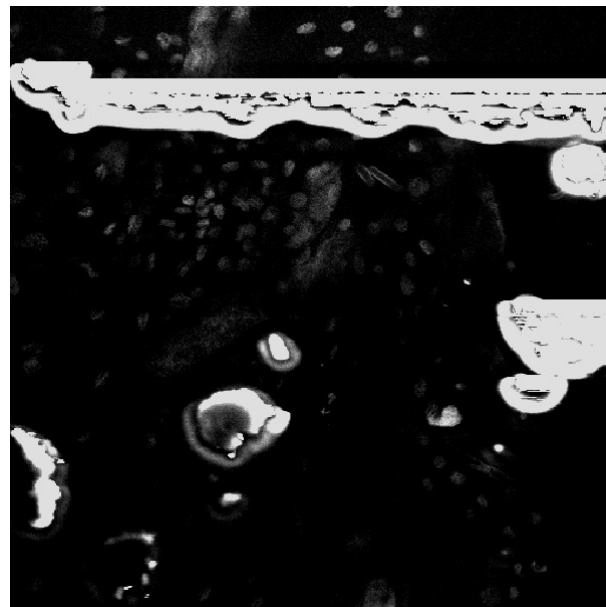


**Fig. 8-15** Bubbles have formed in the mounting media of a fixed sample of a moth embryo. The embryo was labeled with DiA, but the specific signal is obscured by the artifact produced. Sample courtesy of Patty Jansma, University of Arizona.

## 8.4 Troubleshooting Checklist

Several key things can go wrong when imaging that will result in poor or no image being produced. Below is a checklist to help the user produce the best images possible.

### 8.4.1 No image being produced

Laser mode-lock:

Check to see if the laser is turned on and that it is mode-locked. Be sure that the ML-CW- $\beta$ -lock switch on the MIRA controller is set to ML. There should be no filled boxes next to the CW  on the MIRA controller LED readout. If the readout shows CW  then the laser is not mode-locked and no multiphoton excitation can occur. Similarly, there should be a nice bell-shaped curve on the oscilloscope from the Rees Spectrum Analyzer when the laser is mode-locked. A sharp spike anywhere on the Rees Analyzer display is an indication of CW operation. To eliminate CW breakthrough, optimize mode-lock as described in Section 8.3.2.

AOM not on or too little laser power:

Check to see if the laser is turned on in the laser control panel and that the box is checked next to the percent transmission slider. If no image is seen and the laser is on, check the gain on the PMT and then increase the laser power. Determine if the wavelength of the laser matches the wavelength setting on the AOM. Check to see if increasing the percent transmission increases the power to the sample (use the monitor diode) in a linear way. If not, the AOM settings may need to be reset using the "linearize AOTF" macro.

Inefficient fluorochrome excitation (see 8.3.5):

Use a control slide to determine if the problem is in the sample. If excitation is seen with other samples, optimization of the laser wavelength may be necessary.

Laser power to the sample. Verify that the laser is focused through the objective by placing a white card on the microscope stage and removing the objective.

A bright red spot approximately 5-7 mm wide should be seen on the white card.

If no light is seen, then the beam may not be focused into the scan head or the shutter of the AOM may be closed. Check to see if there is a normal level of power going into the scan head. If no beam can be found entering the scan head, the shutter or the AOM may not be working and a service engineer should be called. If there is a beam after the 1 m lens, there may be poor alignment going into the scan head. Report this to a service engineer or attempt realignment under the guidance of a service engineer or expert user. Partial illumination of the card reflects poor alignment and the beam should be realigned into the scan head.

Non-linear power attenuation:

If changing the percent transmission leads to non-linear power attenuation, the AOM can be linearized using the AOTF fit macro. By opening this macro and following the instructions, one can verify the linearization of any of the laser lines and then run a linearization protocol to reoptimize the settings. Be sure the laser is set to the appropriate wavelength before running this macro. Choose only the NIR wavelength to optimize the AOM attenuation for the Ti: Sapphire laser.

#### **8.4.2 Poor image quality**

Lines or spaces across the image:

This can result from an unstable mode-lock. CW breakthrough appears as blank lines in the image. Q-switching will result in wavy lines in the image. The laser must be adjusted to produce stable mode-lock. Check the output from the Rees Spectrum Analyzer and the Optima on the Laser power box. Re-adjust the laser to a stable mode-lock is produced (see 8.3.2.2).

Poor fluorescence sensitivity:

This can result from many factors or a combination of factors. These include the following:

Correct wavelength (see 8.3.5):

Be sure that the laser is set at the best wavelength for the fluorochrome being examined. Empirical testing may be necessary to determine the best wavelength. Tuning to a different wavelength may also help to reduce autofluorescence from some tissues.

Poor Beam Alignment into the scan head (see 8.3.3.2):

Remove the objective and look at the reflection of the beam onto a white card. The beam should be round and even without any flat edges. Peak the alignment of the beam into the scan head.

Poor transmission through the objective (see 8.3.4):

Many objectives are corrected for work with UV and visible range excitation and have poor transmission of photons in the near IR.

## MULTIPHOTON LASER SCANNING MICROSCOPY Troubleshooting Checklist

Carl Zeiss

LSM 510 NLO

---

Poor power output from the laser (see 8.3.2):

Using a power meter check to see if the power output for the laser is in a normal range. The laser is supplied with details about the optimum power output. A very poor power output may be a sign of misalignment of the laser and will affect mode-locking. To peak the alignment, first try to make small adjustments in M7. This will usually restore power to a peak level. You may also need to readjust the BP2 GVD prism and/or the slit width to mode-lock the laser. Make cautious and conservation changes as it is possible that re-alignment of the laser may uncouple the laser from the AOM.

 DO NOT CHANGE THE HORIZONTAL POSITION OF THE SLIT.

Bandwidth too large (see 8.3.2.4):

Minimal bandwidth (6-8 nm) is preferred for this system. Although the laser is capable of producing a mode-locked pulse of up to 12 nm, a pulse with a band width this large will be subject to significant Group Velocity Dispersion (GVD) and result in a longer pulse length at the sample than a pulse with a shorter bandwidth. A longer pulse length at the sample will result in less excitation per unit of average overall power.

Sliders/polarizers in the path:

DIC sliders and polarizers in the path can reduce excitation and emission sensitivity. Remove sliders or slide them to an open position.

Poor sensitivity in fixed samples:

Fixatives and mounting medias can sometimes limit the sensitivity of fluorescence detection or increase autofluorescence reducing the signal-to-noise ratio. For multiphoton excitation, the mounting media can also reduce the peak intensity of the laser deep into the sample. Empirical determination of the best fixative and mounting media for a particular application may be necessary.

## 8.5 References

Albota, M., Beljonne, D., Bredas, J.L., Ehrlich, J.E., Fu, J.Y., Heikal, A.A., Hess, S.E., Kogej, T., Levin, M.D., Marder, S.R., McCord-Maughon, D., Perry, J.W., Rockel, H., Rumi, M., Subramaniam, C., Webb, W.W., Wu, X.L., Xu, C. Design of organic molecules with large two-photon absorption cross sections. *Science* 281, 1653-1656.

Diels, J.C. and Rudolph, W. (1995) *Ultrashort Laser Pulse Phenomena: fundamentals, techniques, and applications on a femtosecond time scale*, San Diego: Academic Press Inc.

Haugland, R. (1996) *Handbook of Fluorescent Probes and Research Chemicals*. M.T.Z. Spence, ed., Eugene, OR: Molecular Probes.

Patterson, G. H. and Piston, D. W. (2000) Photobleaching in two-photon excitation microscopy. *Biophys. J.* 78, 2159-2162.

Kempe, M. (1993) Impact of chromatic and spherical aberration on the focusing of ultrashort light pulses by lenses, *Opt. Lett.* 18, 137-139.

König, K., Simon, U., Halbhuber, K-J (1996) 3D Resolved Two-Photon Fluorescence Microscopy of Living Cells Using a Modified Confocal Laser Scanning Microscope, *Cellular and Molecular Biology* 42, 1181-1194.

Netz, R., Feurer, T., Wolleschensky, R. and Sauerbrey, R. (2000) Measurement of the pulse-front distortion in high numerical aperture lenses, *Appl. Phys. B-Lasers*, 70,833-837.

Rumi, M., Ehrlich, J.E., Heikal, A.A., Perry, J.W., Barlow, S., Hu, Z, McCord-Maughon, D., Parker, T., Röckel, H., Thayumanavan, S., Marder, S., Beljonne, D and Brédas J-L. (2000) Structure-Property Relationships for Two-Photon Absorbing

Chromophores: Bis-Donor Diphenylpolyene and Bis(styryl)benzene Derivatives *J. Am. Chem. Soc.* 122, 9500-9510.

Squirrell, J.M., Wokosin, D.L., White, J.G. and Bavister, B.D. (1999) Long-term two-photon fluorescence imaging of mammalian embryos without compromising viability. *Nature Biotechnology* 17, 763-767.

MULTIPHOTON LASER SCANNING MICROSCOPY  
References

Carl Zeiss

LSM 510 NLO

---

Wolleschensky, R., Feurer T., Sauerbrey R., and Simon I. (1998) Characterization and optimization of a laser-scanning microscope in the femtosecond regime. *Applied Physics B-Lasers and Optics* 67, 87-94.

Wolleschensky, R., Dickinson, M.E. and Fraser, S.E. (2002) Group-Velocity Dispersion and Fiber Delivery in Multiphoton Laser Scanning Microscopy. In, *Confocal and Two-photon Microscopy: Foundations, Applications, and Advances*. Ed. A. Diaspro. New York: Wiley-Liss, Inc.

Xu, C. (2000) Two-photon Cross Sections of Indicators. In, *Imaging Neurons: A Laboratory Manual*. R. Yuste, F. Lanni, and A Konnerth, eds. Cold Spring Harbor, NY: Cold Spring Harbor Laboratory Press.

Recommended Books and Reviews:

*Handbook of Biological Confocal Microscopy* (1995) ed. J. Pawley, New York: Plenum Press.

*Imaging Neurons: A Laboratory Manual*. R. Yuste, F. Lanni, and A Konnerth, eds. Cold Spring Harbor, NY: Cold Spring Harbor Laboratory Press.

*Methods in Cellular Imaging*, A. Periasamy, ed., Oxford, UK: Oxford University Press

Denk, W. and Svoboda, K. (1997) Photon Upmanship: Why Multiphoton Imaging Is More than a Gimmick. *Neuron*, 18,351-357.